Received: 12 February 2021 | Revised: 3 August 2021 | Accepted: 24 September 2021

DOI: 10.1002/ajpa.24431

RESEARCH ARTICLE

AMERICAN JOURNAL OF BIOLOGICAL ANTHROPOLOGY

WILEY

Simulated patterns of mitochondrial diversity are consistent with partial population turnover in Bronze Age Central Europe

Nicolas Broccard[1] | Nuno Miguel Silva[1] | Mathias Currat[1,2]

[1]Laboratory of Anthropology, Genetics and Peopling History, Department of Genetics and Evolution – Anthropology Unit, University of Geneva, Geneva, Switzerland

[2]Institute of Genetics and Genomics in Geneva (IGE3), University of Geneva, Geneva, Switzerland

Correspondence
Mathias Currat, Laboratory of Anthropology, Genetics and Peopling History, Department of Genetics and Evolution – Anthropology Unit, University of Geneva, 1205 Geneva, Switzerland.
Email: mathias.currat@unige.ch

Funding information
Universite de Geneve; Swiss National Science Foundation, Grant/Award Numbers: 31003A_182577, 31003A_156853

Abstract

Objectives: The analysis of ancient mitochondrial DNA from osteological remains has challenged previous conclusions drawn from the analysis of mitochondrial DNA from present populations, notably by revealing an absence of genetic continuity between the Neolithic and modern populations in Central Europe. Our study investigates how to reconcile these contradictions at the mitochondrial level using a modeling approach.

Materials and Methods: We used a spatially explicit computational framework to simulate ancient and modern DNA sequences under various evolutionary scenarios of post Neolithic demographic events and compared the genetic diversity of the simulated and observed mitochondrial sequences. We investigated which—if any—scenarios were able to reproduce statistics of genetic diversity similar to those observed, with a focus on the haplogroup N1a, associated with the spread of early Neolithic farmers.

Results: Demographic fluctuations during the Neolithic transition or subsequent demographic collapses after this period, that is, due to epidemics such as plague, are not sufficient to explain the signal of population discontinuity detected on the mitochondrial DNA in Central Europe. Only a scenario involving a substantial genetic input due to the arrival of migrants after the Neolithic transition, possibly during the Bronze Age, is compatible with observed patterns of genetic diversity.

Discussion: Our results corroborate paleogenomic studies, since out of the alternative hypotheses tested, the best one that was able to recover observed patterns of mitochondrial diversity in modern and ancient Central European populations was one were immigration of populations from the Pontic steppes during the Bronze Age was explicitly simulated.

KEYWORDS
ancient DNA, demographic fluctuation, N1a mitochondrial haplogroup, plague, Yamnaya

1 | INTRODUCTION

The field of ancient DNA is fast evolving and have shed some understanding on the movements of modern humans during Prehistory (e.g., Allentoft et al., 2015; Haak et al., 2015; Hofmanova et al., 2016; Unterlander et al., 2017). However, and while mitochondrial DNA was the first part of our genome to be amplified from human archeological remains, it is very rarely considered in current studies investigating the genetic relationship of ancient and modern populations. More specifically, little has been made to investigate how to reconcile early

observations based on the comparison of mitochondrial DNA (mtDNA) diversity of ancient and modern population samples with current hypotheses of population movements in Europe. In this context, Central Europe was one of the first regions yielding early Neolithic DNA samples (Haak et al., 2005). The analysis of these 24 Neolithic mtDNA from Germany, Austria and Hungary dated from the Linearbandkeramik (LBK) or Alföldi Vonaldiszes Kerámia (AVK) cultures (7500–7000 years ago, kya) showed a surprisingly high frequency of single nucleotide changes (SNPs) characteristic of the mtDNA haplogroup N1a in comparison to modern European populations. The observed frequency of the N1a haplogroup in this ancient sample was 25%, about 150 times more than its current frequency in modern Europeans (Haak et al., 2005). It has since been confirmed that N1a is relatively frequent in early Neolithic samples from Western Europe (around 12% of LBK samples, Brandt et al., 2015; Haak et al., 2010) but rare nowadays in European populations (less than 1%, Brandt et al., 2015; Fu et al., 2012). The mitochondrial haplogroup N1a is believed to have appeared in the Near East (Richards et al., 2000) between 12 and 32 kya years ago (Palanichamy et al., 2010) and to have been introduced by the first farmers who entered Europe during the Neolithic transition (Brandt et al., 2013, 2015; Haak et al., 2010) possibly through a leap-frog colonization process (Palanichamy et al., 2010). It is considered as a marker of early farmer groups in Central and Western Europe (Haak et al., 2005, 2010; Rivollat et al., 2016) and has been found in Hungary (Gamba et al., 2014; Szecsenyi-Nagy et al., 2015), Germany (Brandt et al., 2013; Haak et al., 2005, 2010), the Paris area (Rivollat et al., 2015), the Iberic peninsula (Lipson et al., 2017) and the Atlantic coast (Deguilloux et al., 2011). The decrease in N1a frequency from the Neolithic to the present has been interpreted as an evidence that the first farmers in Central Europe failed to leave a genetic signal on the matrilineal side of modern Europeans (Haak et al., 2005). In this latter study, simulations showed that such a change in N1a frequency could not have been caused by genetic drift alone, supporting the hypotheses that either farming spread by cultural diffusion from relatively small pioneer farmer groups carrying N1a to local hunter-gatherers not carrying this haplogroup, or that a population replacement occurred in Europe after the Neolithic expansion. The latter hypothesis has found further support from other studies showing strong genetic differentiation between Neolithic and modern mtDNA samples in Central Europe (Bramanti et al., 2009; Silva et al., 2017). This has been interpreted as a lack of continuity between the Neolithic and current human populations in this region, where "population continuity" refers to genetic drift being able to account for the change of genetic diversity from one time period to the next. An absence of population continuity could result from a partial population turnover, which tends to increase the genetic differentiation between the samples drawn from distinct periods before and after the turnover (Ortega-Del Vecchyo & Slatkin, 2019).

The hypothesis of this population turnover between the Neolithic and the present contrasts with previous findings based on mtDNA of modern European populations. For instance, mismatch distributions (i.e., the distribution of differences between all pairs of sequences taken from a population sample) computed in modern populations from Central Europe are mostly smooth and unimodal (Excoffier & Schneider, 1999), indicative of an ancient population expansion (Excoffier, 2004; Ray et al., 2003), estimated to have occurred some 40 kya (Comas et al., 1996; Excoffier & Schneider, 1999). This would thus correspond approximately to the arrival of the first *Homo sapiens* on the European continent. Indeed, it was shown that recent reduction in population size, recent bottleneck or partial population replacement can alter the signal of past population expansions in the mismatch distribution (Currat & Excoffier, 2005; Excoffier & Schneider, 1999; Rogers & Harpending, 1992). We would therefore expect that population discontinuity between Neolithic and modern Europeans due to a substantial population replacement would also have altered the unimodal shape of the mismatch distribution generally observed in modern European populations (Excoffier & Schneider, 1999).

At least four alternative (not mutually exclusive) hypotheses could have caused shifts in allele frequencies in Central European populations leading to an increased genetic differentiation between Neolithic and modern population samples: (1) genetic drift since the Neolithic until the present (i.e., during the last 7 kya); (2) fluctuations in population sizes at the beginning of the Neolithic transition (i.e., around 7000 BP); (3) high death rates decimating European populations during historical period as results of epidemics (i.e., after 2000 BP); (4) partial replacement of Central European gene pool due to immigration from another area, subsequently to the Neolithic transition (i.e., sometime between 7000 BP and the present). This latter explanation has recently gained support by paleogenomic data indicating a significant genomic input of populations associated to the Yamnaya cultural complex from the Pontic steppes during the Bronze Age (approximately between 6500 and 4800 BP, Allentoft et al., 2015; Haak et al., 2015). Although this period is culturally complex, to keep the text simple we will hereafter use the term "Yamnaya" to refer to those Bronze Age populations migrating toward Central Europe from the East.

The patterns of genetic diversity expected in complex spatio-temporal processes of population movement and admixture are difficult to predict with simple mathematical models. The spatially explicit simulation framework offers a powerful tool to address this problem as it can account for population dynamics in space and time and more specifically for population structure, migration, and interactions. It was used to describe important evolutionary processes taking place during population expansions (e.g., Currat et al., 2008; Klopfstein et al., 2006; Ray et al., 2003). Regarding human evolution in the European continent, this approach has been mostly applied to the period going from the early colonization of the continent by modern humans until the Neolithic transition (e.g., Arenas et al., 2013; Currat & Excoffier, 2005; Rasteiro et al., 2012), but rarely to more recent periods, at the notable exception of Barbujani et al. (1995) and Rendine et al. (1986), who applied simulation of allele frequencies to migrations from the Eastern steppes after the Neolithic. Our study improves this approach by explicitly investigating the effect of various types of post Neolithic demographic events in a spatial context on

both modern and ancient mtDNA. Furthermore and in opposition to an earlier study aiming at exploring the effect of genetic drift on the frequency of N1a (Haak et al., 2005), our simulation approach account for population structure and migration, which have been shown to substantially affect ancient DNA analysis (Silva et al., 2017).

In order to reconcile these apparent contradictions in observed patterns of mtDNA genetic diversity between Neolithic and modern population samples from Central Europe, we investigated whether any of the four alternative hypotheses described above can generate the observed patterns. To do so, we simulated ancient and modern mitochondrial diversity in Central Europe under these four different hypotheses, and then compared statistics of genetic diversity computed on simulated and observed data in order to evaluate the plausibility of the scenarios. Our objective was to identify which scenarios—if any—may result in both a large genetic differentiation between Neolithic and present populations, as quantified by the *Fst* statistics (Bramanti et al., 2009; Haak et al., 2005), and a uniform mismatch distribution in present population. We also considered the change in frequency of simulated haplogroups similar to N1a and investigated if a decrease in frequency as large as the one observed for this haplogroup between the Neolithic and the present can be expected under any of the various scenarios simulated.

2 | MATERIAL AND METHODS

2.1 | Observed statistics used for comparison with simulated data

To assess the plausibility of the simulated scenarios, we compared the simulated data to previously published mitochondrial data. Table 1 synthesizes the observed and simulated data used to assess the fit between them.

In order to investigate the diversity at the HVS1 mitochondrial region, our study uses 25 Neolithic mtDNA sequences from Central Europe published in Bramanti et al. (2009); 101 modern mtDNA sequences from the same region (Germany) published in Baasner and Madea (2000) and retrieved from the HvrBase++ database (Kohl et al., 2006). The observed statistics computed on this published data are the *Fst* between the Neolithic and the modern mtDNA sample ($Fst = 0.072$, P-value $<10^{-6}$) and the mismatch distribution computed on the modern sample.

In order to estimate the diversity of the N1a haplogroup, we computed the nucleotide diversity (=0.002) in a random subset of 17 mitogenomes belonging to this haplogroup and retrieved from the public database phylotree.org, version 19.02.2014 (van Oven & Kayser, 2009). The most differentiated pair of N1a mitogenomes in this subset differs by 39 positions over the 16576 bp, which is used as a reference to simulate mtDNA haplogroups of genetic diversity similar to the one observed for N1a (see below). In addition, we used the frequencies of the haplogroup N1a estimated by Brandt et al. (2015) for the Neolithic period from 109 LBK individuals (11.9%) and in modern-day Eurasian populations (<1%).

2.2 | Spatially explicit simulation of ancient and modern mitochondrial DNA

The four hypotheses explained above have been modeled with the program SPLATCHE3 (Currat et al., 2019), a program that allows to simulate (i) forward-in-time demographic changes in a structured

TABLE 1 Description of the observed and simulated statistics used for the evaluation of simulated scenarios

Comparison	Observed data	Simulated data
Modern mismatch distribution in Central Europe.	101 HVS1 modern German mtDNA from (Baasner & Madea, 2000) retrieved from HvrBase++ (Kohl et al., 2006), version October 2015.	101 "modern" mtDNA of 360 bp drawn in four demes from central Europe (shown in Figure 1c) at generation 1679.
Computation of genetic distance ($Fst_{anc\text{-}mod}$) between the ancient and the modern samples in Central Europe.	101 HVS1 modern German mtDNA from (Baasner & Madea, 2000) retrieved from HvrBase++ (Kohl et al., 2006), version October 2015. 25 HVS1 early Neolithic mtDNA from Bramanti et al. (2009).	101 "modern" mtDNA and 25 "Neolithic" mtDNA of 360 bp drawn in four demes from central Europe (shown in Figure 1c) at generation 1679, and 1380, respectively.
Maximum number of differences between sequences belonging to the N1a haplogroup.	Random subset of 17 mitogenomes associated to the haplogroup N1a recovered from phylotree.org (van Oven & Kayser, 2009), version 19.02.2014 (list of mitogenomes available on request).	Simulated haplogroups based on a phylogeny of 600 mitogenomes of 16,070 bp long drawn in four demes from central Europe (shown in Figure 1c): 200 "modern" mitogenomes at generation 1679, 200 "Neolithic" mitogenomes at generation 1380 and 200 additional mitogenomes at generation 1299. The diversity and change in frequency in those haplogroups is then computed.
Change of N1a frequency in Central Europe between the Neolithic and the present.	11,9% in 109 LBK individuals and < 1% in modern-day Eurasian populations (Brandt et al., 2015).	

population divided in demes (sub-populations) distributed over a two dimensional space, then (ii) backward-in-time genetic diversity of samples taken from specific demes (i.e., geographic locations).

SPLATCHE3 simulates the evolution of populations in a virtual map, generation by generation. Here the map represents Western Eurasia (Figure 1) and is divided in geographic cells of 100 x 100 *km*. Each cell contains one (scenarios H0, H1, and H2) or two (scenario H3) demes. The simulation starts 1680 generations in the past (around 42000 years ago using 25 years as generation time, Helgason et al., 2003; Tremblay & Vezina, 2000) from a single deme placed arbitrarily in Anatolia from which migrants eventually colonize the whole map (shown with an X in Figure 1a).

The simulation proceeds in two steps. During the first step, demes increase in density and exchange migrants according to a stepping stone model (Kimura, 1953). The density is regulated by a logistic equation defined by two parameters: the growth rate r and the carrying capacity K as $N_{t+1} = N_t + r\, N_t\left(1 - \frac{N_t}{K}\right)$, where N_t and N_{t+1} are the effective population sizes at generation t and $t+1$, respectively. The carrying capacity of demes was changed at different periods to represent the number of individuals that can be sustained by environmental conditions and technological advances (i.e., hunting and gathering or agriculture, industrial era). Apart from K, all parameters were kept constant during the rest of the simulation. The growth rate has been set to 0.4 as in Currat and Excoffier (2005) and the migration rate to 0.025 to fit the colonization time of Europe by modern humans in approximately 500 generations (Bocquet-Appel & Demars, 2000). During the second step, two mtDNA population samples are simulated using the serial coalescent algorithm implemented in SPLATCHE3. For neutral loci, as assumed here for mtDNA, the coalescent reconstruction is a stochastic process that relies only on the

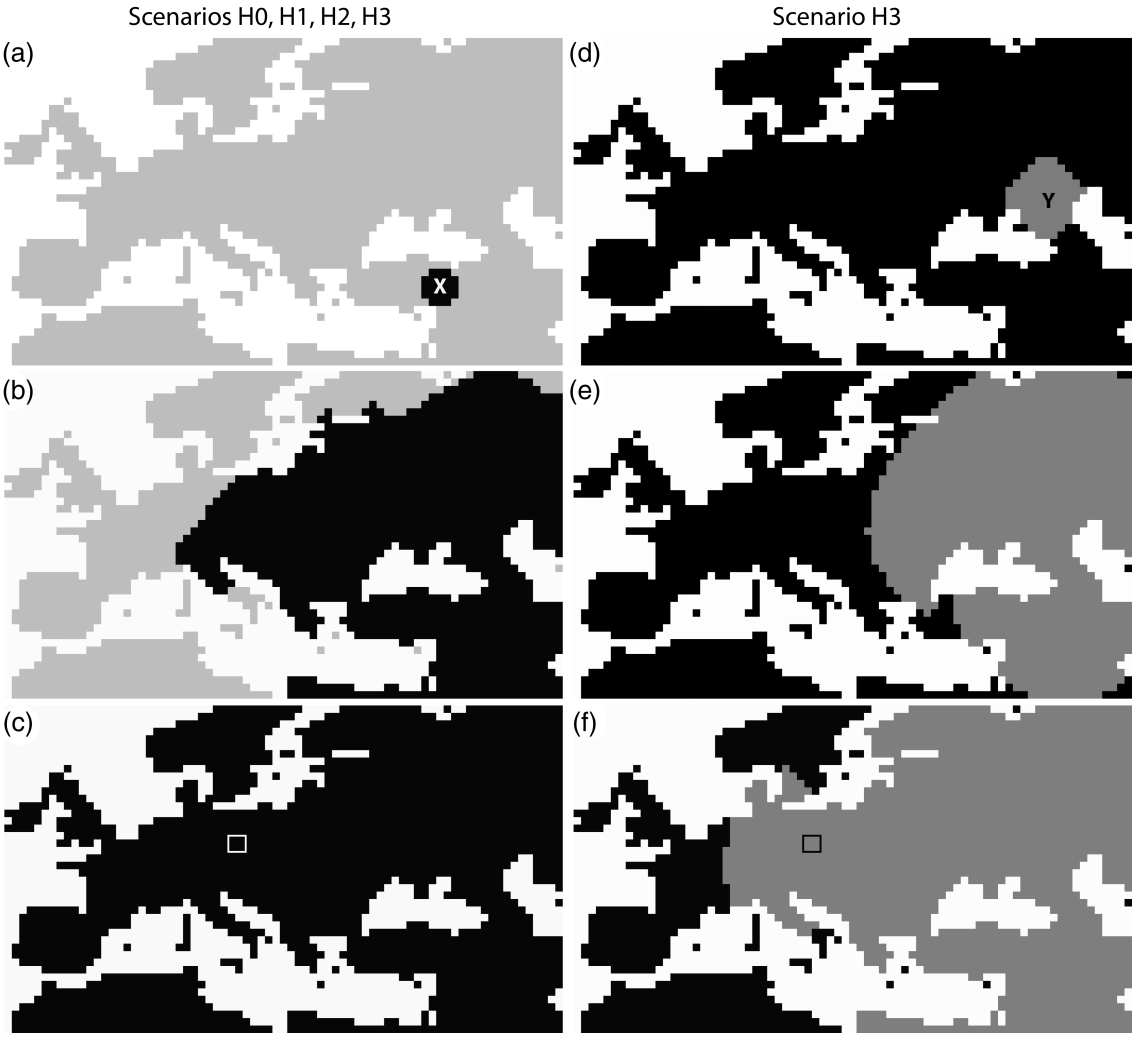

FIGURE 1 Illustration of six consecutive time steps of the simulation scheme. The map of Europe used for the simulations with SPLATCHE3 is made of cells representing 100 x 100 *km*. White represents water cells, light gray represents empty land cells, black represents land cells occupied by humans that started their expansion in deme X, 42000 years before the present. (a–c) Scenarios H0, H1, and H2 uses only this single population layer. (d–f) Scenario H3 uses a second superimposed population layer starting in deme Y at generation 1460. Genetic sampling is done in the four demes of the first population layer represented by the white square on panel C for scenario H0, H1, and H2, and in the four demes of the second population layer represented by the black square on panel F for scenario H3 (same sampling conditions for all scenarios)

densities and migrations simulated during the first step. To approximate the observed sampling locations, both mtDNA samples were drawn from four different demes located in Central Europe (square in Figure 1c,f). The first sample of 25 simulated mtDNA sequences was drawn during the Neolithic period at generation 1380 after the beginning of the simulation. The second simulated sample of 101 mtDNA sequences was drawn at present time, that is, at generation 1680 after the beginning of the simulation. The genetic diversity as measured by (1) the *Fst* between the simulated Neolithic and modern samples and (2) the mismatch distribution in the simulated modern samples were calculated and then compared to those statistics measured in the observed data (see above). The "double layer" option of SPLATCHE3 was used for scenario H3 (see below) allowing simulating two interacting populations exchanging various amounts of gene flow, as analogous to two culturally distinct human populations (Currat & Excoffier, 2005).

2.3 | Scenarios simulated

Four major scenarios were simulated as described below and in Table 2. The input datasets as well as the executable are available in Zenodo with DOI https://doi.org/10.5281/zenodo.5541872. The scenarios were parameterized according to the specific location of the four demes in Central Europe where simulated genetic diversity was sampled, but the same parameter values applied to all demes in the map. There are mainly two related reasons for this choice: (i) in order to optimize computation time and (ii) because estimating parameters, such as growth rates or migration rates of human populations across the European continent, were not of interest to the current study and to address the already parameter-heavy hypotheses simulated here.

H0. Genetic drift in a structured population.

Scenario H0 simulated the evolution of European populations since the arrival of the first anatomically modern humans in Central Europe around 42000 years ago (e.g., Mellars, 2006). We simulated a long-term increase of population density by changing several times the carrying capacity *K* in all demes at once, without any other particular disturbance (Figure 2). At the beginning of the simulation (generation 0), *K* was set to 160 individuals to reflect the census size estimated for hunter-gatherer populations (0.064 individuals per km^2, Alroy, 2001; Steele et al., 1998). Relative to the deme size we used (10,000 km^2), this census size corresponds to 640 individuals per deme, including non-reproductive young and old people. Considering that the effective size represent half of the census size, 640 individuals per deme leads to 320 reproductive individuals and, assuming an equal sex ratio, to 160 females. We used this carrying capacity, since we consider mtDNA and thus we only needed to simulate females. At the onset of the Neolithic transition (generation 1300), the value of *K* was changed to 3200, reflecting the demographic increase due to the domestication of crops and animals (Bocquet-Appel & Dubouloz, 2003). At generation 1508 and at generation 1600, *K* grew up to 7500 and 17500, respectively, thanks to climate warming allowing to sustain larger populations and as evidenced with the start of Antiquity (Bardet & Dupaquier, 1997). Then, at generation 1616, *K* was set to 75000 due to a demographic growth, then to 155000 during the 12^{th} and 13^{th} centuries (generation 1644) and finally to $K = 200000$ at generation 1670, reflecting the industrial—present—era (Bardet & Dupaquier, 1997). This scenario H0 is inspired from to the one originally developed in Haak et al. (2005) but includes the effect of population structure.

H1. Neolithic booms and busts.

TABLE 2 Parameters used for all simulated scenarios with SPLATCHE3. See text for details about the scenarios. *r* stands for the population growth rate, *m* for the migration rate, and γ for the admixture rate.

	Hypotheses	Scenario	Bottleneck dates	r_{FAR}	r_{YAM}	m_{FAR}	m_{YAM}	γ	Genetic replacement
1 Layer	Continuous	H0 (continuous)	-	0.4	-	0.025	-	-	-
	Neolithic fluctuations	H1a (frequent)	1440, 1442, 1444, 1446	0.4	-	0.025	-	-	-
		H1b (long interval)	1440,1450	0.4	-	0.025	-	-	-
		H1c (long duration)	1440 → 1450, 1451 → 1461	0.4	-	0.025	-	-	-
	Historical plague	H2a (50% mortality)	1655, 1662, 1665	0.4	-	0.025	-	-	-
		H2b (90% mortality)	1655, 1662, 1665	0.4	-	0.025	-	-	-
2 Layers	Bronze Age migration	H3a (0% replacement)	-	0.4	0.4	0.025	0.25	0.05	0.003 (0.00–0.02)
		H3b (25% replacement)	-	0.4	0.4	0.025	0.25	0.01	0.272 (0.12–0.44)
		H3c (37.5% replacement)		0.4	0.4	0.025	0.25	0.08	0.369 (0.20–0.52)
		H3d (50% replacement)	-	0.4	0.4	0.025	0.25	0.006	0.479 (0.30–0.64)
		H3e (62.5% replacement)		0.4	0.4	0.025	0.25	0.004	0.645 (0.46–0.80)
		H3f (75% replacement)	-	0.4	0.4	0.025	0.25	0.003	0.723 (0.54–0.86)
		H3g (100% replacement)	-	0.4	0.4	0.025	0.25	0.0	1.000 (1.00–1.00)

Note: The last column shows the exact proportion of genetic contribution from Yamanya to the modern central European gene pool, with its 95% percentile within brackets.

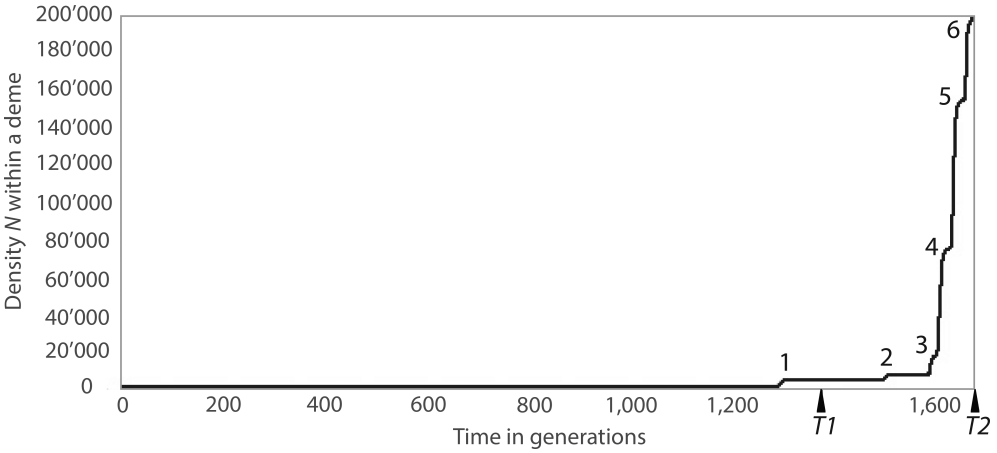

FIGURE 2 Evolution through time of population density N within a deme under scenario H0. Numbers refer to changes in carrying capacities (see text for details) 1: Neolithic transition; 2: Start of antiquity; 3–4: episodes of climate warming; 5: 12th and 13th centuries; 6: Industrial era. *T1* and *T2* represent sampling times in central European demes (square in Figure 1)

Scenario H1 was based on scenario H0 but it simulated the effects of demographic fluctuations which occurred during the Neolithic transition (Shennan et al., 2013; Zimmermann et al., 2009) probably due to climate, diseases or soil erosion. For each drop, K felt from 3200 to 200 in all demes. We chose an extreme value for this density drop (∼95%) in order to maximize the chances of observing an effect on genetic diversity, if any. We simulated three variants of this scenario, which varied by the number and duration of these demographic fluctuations. H1a simulated four demographic fluctuations, separated by 2 generations each (generations 1440, 1442, 1444 and 1446). H1b simulated only two fluctuations separated by 10 generations (at generations 1440 and 1450). Finally, H1c also simulated two demographic fluctuations, as in H1b, but they lasted for longer (5 generations each).

H2. Demographic collapses due to epidemics such as plague during historical time.

Scenarios H2 was based on scenario H0 with the following changes to account for the effects of plague epidemics. For scenario H2a, K decreased at three successive times during one generation to half its value ($K = 75000$) then returned to its previous value of 150000. Those three demographic collapses occurred at generations 1655, 1665 and 1669 and correspond to the three large plague epidemics between 541 AD and 1722 AD (including the black plague in 1375 AD) which decimated up to 80% of the population in certain regions but probably around 30–50% on average for the whole European continent (Livi Bacci, 1999; Biraben, 1979; Eckert, 2000). We tested an extreme version of this scenario, H2b, corresponding to 90% mortality rate by reducing K to 15000.

H3. Migration from the Pontic steppes to Central Europe during the Bronze Age.

Scenario H3 simulated a migration wave from the Pontic steppes during the Bronze Age. This hypothesis was first developed by Gimbutas (1979, 1991) who proposed three successive migration waves between 6500 and 4800 BP and led by populations associated to the "Kurgan" culture, which groups both the "Yamnaya" and "Corded ware" cultures. Despite this hypothesis being still debated among archeologists (e.g., Demoule, 2014), it recently received support from extensive paleogenomic studies (Allentoft et al., 2015; Haak et al., 2015). We represented the immigration of the "Yamnaya" population from the Pontic steppes and their interactions with populations already established in Europe that we refer to as "Farmers" thereafter. We considered both populations as culturally distinct from each other and thus evolving in a separated layer of demes, thereby making use of the "double layer" option of SPLATCHE3. This option allows simulating an additional population group on top of the first layer. The first layer is the same as in H0, H1, and H2. In H3, the Yamnaya population started to spread over the second layer from a single deme located in the Pontic area (shown as Y in Figure 1d). The Yamnaya population then colonized the second layer and admixed with the population of the first layer as follows. Each geographic cell contained two panmictic demes, one representing the farmer population and the other one the Yamnaya population. Gene flow between the two demes was regulated by the admixture rate γ. At each generation, there is a probability A_{ij} for each individual N_i of passing from one deme i to the other deme j, computed as

$$A_{ij} = \gamma(2N_iN_j)/(N_iN_j)^2$$

where N_i and N_j are the density of deme i and j, respectively. N_iA_{ij} is the number of effective genes going from population i to population j at the corresponding generation. This gene flow could be due either to the birth of a female in population j with her parents belonging to population i, or to the assimilation of an individual i in the population j. Both situations would result in the transfer of mtDNA from population i to j. When $\gamma = 0$, no admixture between either populations occured while when $\gamma = 1$ both demes sharing the same cell would be considered as panmictic and would therefore imply extensive gene flow between them. For instance, $\gamma = 0.5$ would mean that reproduction between members of the distinct populations (i.e., Yamnaya in layer 2 and farmers in layer 1) occurred half as often as reproduction between members of the same population. We used the admixture

model called "assimilation" in SPLATCHE3 as described in details in Currat and Excoffier (2005).

To account for different amount of genetic contribution from the Yamnaya to the modern local gene pool, we simulated seven different variations of scenario H3 with different values of γ (0.0, 0.003, 0.004, 0.006, 0.008, 0.01, and 0.05). As shown in Figure 3, those values of γ correspond approximatively to a genetic contribution of Yamnaya of 100, 75, 62.5, 50, 32.5, 25, and 0%, respectively, at the end of the simulation in the four demes where the sampling is done (square in Figure 1f). In absence of further information, γ is identical in both direction (from Yamnaya to Farmers and the opposite). We did not explore $\gamma > 0.05$ further because it always led to a final genetic contribution of Yamnaya equal to 0% as admixture was in this situation high enough for the Yamnaya genes to be fully "diluted" in the farming population before reaching Central Europe (Figure 3). This is a well-known process in the context of the Neolithic transition (Chikhi et al., 2002; Silva et al., 2018), which has also been described to occur commonly in the situation of biological invasions with admixture (Quilodran et al., 2020).

For all variation of scenario H3, the Yamnaya population emerged in northern Caucasus (Y in Figure 1) at generation 1460 (~8550 BP) and the migration rate was set to 0.25 to reproduce a migration wave reaching Central Europein about 1000 years, which is approximately when the Yamnaya genomic contribution starts to be detected in Central Europe (Allentoft et al., 2015; Haak et al., 2015). To avoid setting different demographic parameters for Yamnaya and Farmers in absence of further knowledge, and because this would be beyond the scope of the current objectives, we assumed an absence of resource competition between them. This implies that Yamnaya and Farmers cohabit in the same cell without hindering each other until the end of the simulation. Both populations have thus the same growth rate *r* and carrying capacity *K*. Using the model of direct competition implemented in SPLATCHE3 would require setting different parameters for both layers.

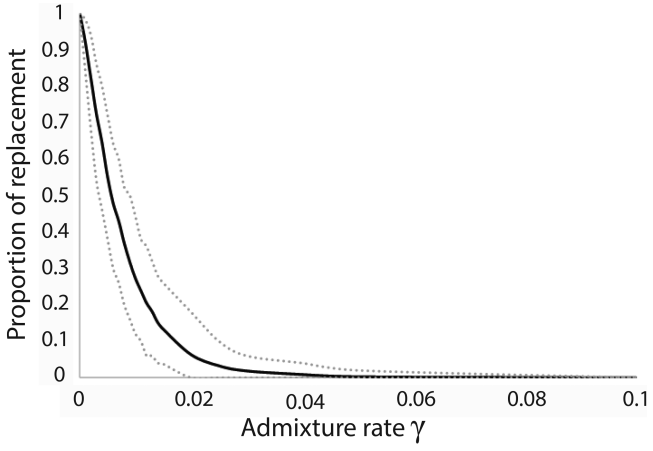

FIGURE 3 Proportion of genetic replacement in Central Europe during the Bronze Age depending on the rate of admixture used under scenario H3 (mean and 95% percentile for 1000 simulations)

2.4 | Coalescent reconstruction

Once the demographic simulation is achieved, a genealogy is reconstructed for a series of samples drawn from two generation times and from four neighboring demes located in Central Europe (see Figure 1c,f), until their most recent common ancestor (MRCA). The two generation times when sampling occurred aimed to represent the "Neolithic" (generation 1380, referred to *T1* in Figure 2) and the present ("modern," generation 1679 referred to *T2* in Figure 2). For neutral loci, this coalescent reconstruction is stochastic and depends only on the demography of the population simulated during the demographic step. See the original description of SPLATCHE for more details on the algorithm (Currat et al., 2004).

The genetic diversity of these simulated samples was generated by spreading mutations over the coalescent tree, as expected under the neutral coalescent. For HVS1 region, we simulated 25 "Neolithic" mtDNA sequences and 101 "modern" mtDNA sequences of 360 bp each using a mutation rate $\mu = 1.32*10^{-7}$ per site per generation (Ray et al., 2003). These sample sizes correspond to those sizes of the observed samples (see Table 1). Using the same approach, we also simulated 600 mitogenomes including 200 "Neolithic," 200 "modern," and 200 additional taken at generation 1299. This last sample was only set to get enough resolution for the phylogenetic reconstruction and the frequency of the simulated haplogroups in this sample was not recorded. Following Rieux et al. (2014), we allowed for heterogeneous mutation rates along the mitogenome and divided it into four blocks, on 7565 sites $\mu = 1.89*10^{-7}$, on 3776 sites $\mu = 8.31*10^{-7}$, on 698 sites $\mu = 7.858*10^{-6}$, on 4031 sites $\mu = 2.58*10^{-7}$.

2.5 | Haplogroup simulation

For each simulation, the 600 mitogenomes were first classified by maximum parsimony on a phylogenetic tree using RAxML (Stamatakis, 2014) and later analyzed using a homemade script written in Python. The branches of the phylogenetic tree were explored starting from the root to identify the most basal nodes from which derived branches had no more than 39 pairwise differences, as observed in a sample of modern mitogenomes associated to the N1a haplogroup. If the branches derived from the current node had 39 differences at most, then all branches issued from this node were considered to belong to a haplogroup of similar diversity to N1a, and the algorithm moved to the next basal node, if any. This was repeated until all terminal branches had been assigned to an haplogroup. The frequency of the simulated haplogroup was then calculated for the two sampling periods of interest ("Neolithic" and "modern" with $n = 200$ for each sample). For each scenario, we computed the proportion P_{Na1} of simulated haplogroup among 1000 simulations for which the frequency dropped at least in the proportions observed between Neolithic and modern Central European populations (from ≥12% in Neolithic to ≤1% in modern time, Table 1).

2.6 | Statistical analysis

The program Arlequin (Excoffier & Lischer, 2010) was used to compute the *Fst* statistic measuring genetic differentiation between the "Neolithic" and the "modern" sample in Central Europe, as well as the mismatch distribution in the modern sample, both for the simulated and observed data (Table 1). A mismatch distribution $f(x)$ was considered unimodal if it is monotonically increasing for $x < m$ and monotonically decreasing for $x > m$, $f(m)$ being the maximum value of $f(x)$. These were criteria assessed in the mismatch distributions of the simulated samples using a homemade script written in Python. We ran it on the observed mismatch distribution of the modern sample, which was found unimodal ($P < 10^{-6}$), similarly to most mismatch distributions computed for modern European populations (Excoffier & Schneider, 1999). For each scenario, we computed the proportion of 1000 simulation with unimodal mismatch distribution (P_{uni}) and the average *Fst* between the ancient and the modern sample ($Fst_{anc\text{-}mod}$). We also computed the proportion ($Fst_{sim>obs}$) of 1000 simulations that gave a simulated *Fst* larger than the observed *Fst*. In addition, we report the proportion of simulations leading to both a unimodal mismatch distribution and a *Fst* as large as the one observed (P_{uni} and $Fst_{sim>obs}$). Excepted for the $Fst_{anc\text{-}mod}$ statistics, for which the average value is given, we decided that each other statistics computed as a proportion was not compatible with the observed data if its probability to reproduce the observed pattern was smaller than 5%, meaning that the scenario is unlikely to reproduce the observed statistics.

3 | RESULTS

As shown in Table 3, the scenario H0 of population continuity in a subdivided population is unable to explain all observed patterns of diversity at the mitochondrial level. It shows an unimodal distribution compatible with the observation (shown by dotted lines in Figure 4) in 96% of the simulations (P_{uni}), but it is unable to explain the large observed genetic differentiation ($Fst = 7.2\%$, see Section 2) between the Neolithic and present samples as the mean *Fst* is 0.31% with only 0.2% ($Fst_{sim>obs}$) of simulations producing a *Fst* larger than the observed value. Finding a drop in haplogroup frequency between Neolithic and modern samples as large as the one observed for N1a is rare but possible ($P_{Na1} = 6.0\%$).

The scenarios H1 of demographic fluctuation during the Neolithic shows very similar results to H0 with most mismatch distributions being unimodal ($P_{uni} > 93\%$), a low mean *Fst* ($Fst_{anc\text{-}mod} \leq 0.44\%$), a maximum of 0.3% of *Fst* as large as the observed value. Between 5.2 and 8.2% (P_{Na1}) of simulated haplogroups show a frequency drop similar to the one observed for N1a. Even though we simulated demographic fluctuations with a large amplitude (90% reduction) and different durations; the outcomes of the H1 scenarios do not differ much from those produced under a continuous population growth (H0).

The scenarios H2 simulating the effects of plague shows outcomes comparable to those of H0 and H1, even though it modeled three major population drops during historical time. It results in a large majority of unimodal mismatch distributions ($P_{uni} > 96\%$), a low mean *Fst* ($Fst_{anc\text{-}mod} \leq 0.3\%$), a very low proportion of *Fst* as large as the observed one ($Fst_{sim>obs} \leq 0.4\%$) and a low proportion of haplogroups behaving similarly to N1a ($P_{Na1} \sim 5$–6%).

The scenarios H3 simulating a genetic input during the Bronze Age due to a population expansion from the Pontic steppes and partial replacement of Central European populations give contrasting results depending on the admixture rate. Scenario H3a simulated the largest admixture rate, which lead to full mixing between both populations (i.e., Yamnaya and Farmers) and resulted in the absence

TABLE 3 Results (in %) obtained for all simulated scenarios, 1000 simulations per scenario.

	Hypotheses	Scenario	$Fst_{anc\text{-}mod}$	$Fst_{sim>obs}$	P_{uni}	P_{uni} & $Fst_{sim>obs}$	P_{N1a}
1 Layer	Continuous	H0 (continuous)	0.31 (0.0–3.34)	0.2	96.0	0.2	6.0
	Neolithic fluctuations	H1a (frequent)	0.37 (0.0–3.40)	0.2	95.6	0.2	5.5
		H1b (long interval)	0.30 (0.0–2.94)	0.2	93.6	0.1	7.2
		H1c (long duration)	0.44 (0.0–3.51)	0.3	94.6	0.3	8.2
	Historical plague	H2a (50% mortality)	0.30 (0.0–3.44)	0.3	96.2	0.1	5.7
		H2b (90% mortality)	0.25 (0.0–2.83)	0.4	96.7	0.5	5.2
2 Layers	Bronze Age migration	H3a (0% replacement)	0.76 (0.0–4.07)	0.4	96.6	0.4	17.8
		H3b (25% replacement)	1.07 (0.0–4.58)	1.1	94.3	0.0	39.0
		H3c (37.5% replacement)	6.81 (1.14–16.69)	38.7	74.7	23.0	42,9
		H3d (50% replacement)	9.69 (1.71–23.01)	60.6	53.0	24.6	50.0
		H3e (62.5% replacement)	13.24 (2.52–28.54)	78.0	32.7	19.8	61.7
		H3f (75% replacement)	19.23 (4.49–39.48)	92.2	16.4	12.8	69.5
		H3g (100% replacement)	36.64 (9.60–70.31)	98.9	12.2	11.7	99.7

Note: *Fstanc-mod is the mean Fst computed between the ancient and the modern sample, with its 95% percentile within parentheses*. $Fst_{sim>obs}$ is the proportion of simulated *Fst* between Neolithic and modern samples larger that the observed one ($Fst_{obs} = 7.2\%$). P_{uni} is the proportion of unimodal mismatch distributions. P_{uni} and $Fst_{sim>obs}$ are the proportion of simulations giving both a unimodal distribution and a *Fst* as large as observed. P_{N1a} is the proportion of simulated haplogroups equivalent in diversity to N1a showing a similar drop in frequency between the Neolithic and modern time.

of genetic replacement in Central Europe. It gave similar results to scenarios H0, H1 and H2, with a majority of unimodal mismatch distributions ($P_{uni} = 96.6\%$), low genetic differentiation ($Fst_{anc\text{-}mod} = 0.76\%$, $Fst_{sim>obs} = 0.4\%$), but a substantially larger proportion of haplogroups dropping in frequency as N1a ($P_{Na1} = 17.8\%$). At the other extreme, the scenario H3g has an admixture rate equal to zero leading to a full

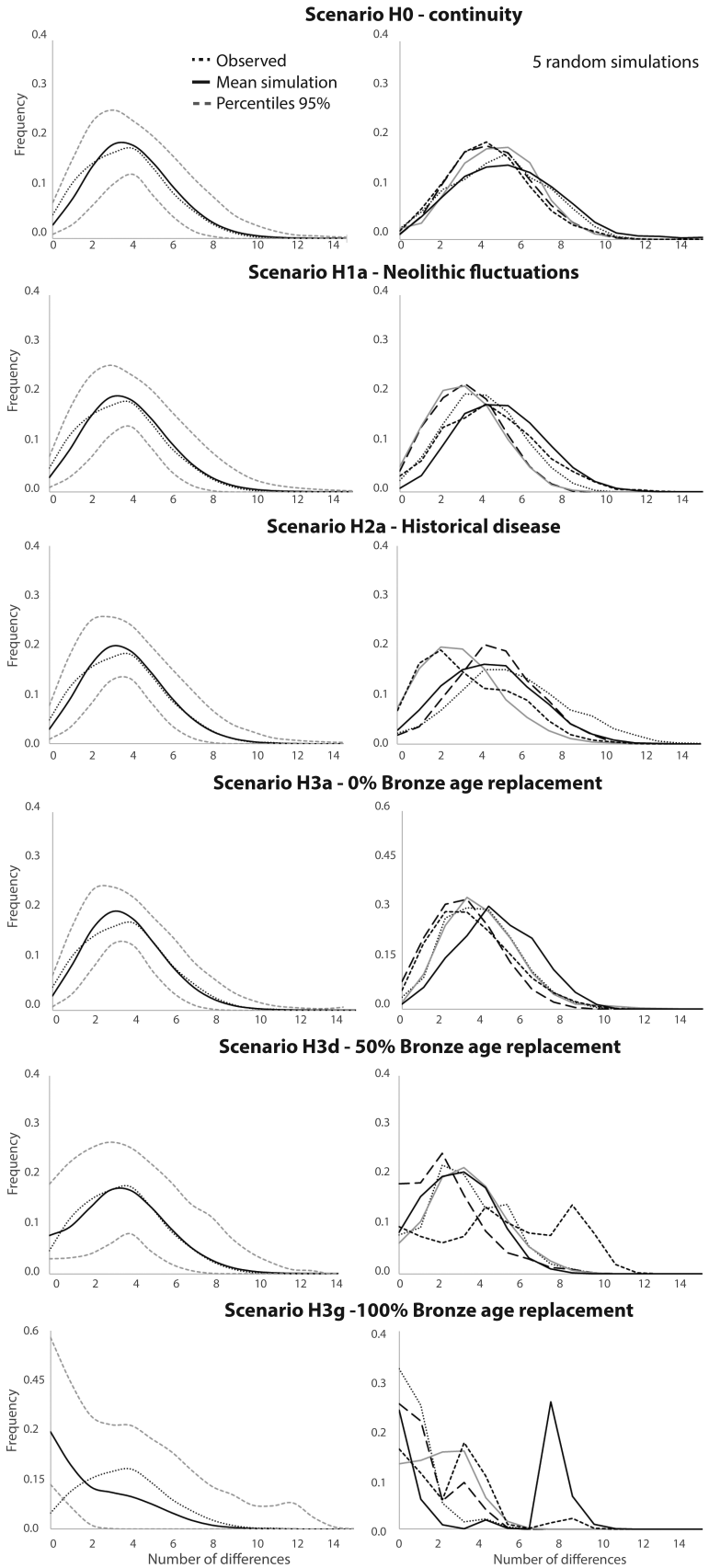

FIGURE 4 Mismatch distributions simulated under six different scenarios. The left column shows the mean (black line) and percentiles 95% (dotted lines) for 10000 simulations, as well as the observed mismatch distribution in a modern sample from Germany (dash line). The right column shows five examples randomly chosen for each scenario

replacement of the Central European genetic pool by the migrating populations from the Pontic steppes. H3g results to the opposite pattern than H3a with a low proportion of unimodal mismatch distribution ($P_{uni} = 12.2\%$), a large genetic differentiation among sampling periods ($Fst_{anc\text{-}mod} = 36.64\%$, $Fst_{sim>obs} = 98.9\%$) and a very high proportion of simulated haplogroups dropping in frequency as N1a ($P_{Na1} = 99.7\%$).

Under scenario H3, the proportion of unimodal mismatch distributions decreases with the amount of genetic replacement during the Bronze Age, while the genetic differentiation between the Neolithic and the modern samples increases, as expected. All versions of scenario H3 show higher proportions of simulated haplogroups presenting the same pattern to the one observed for Na1, compared to the other scenarios H0, H1, and H2.

Figure 4 shows that the mean mismatch distributions obtained under scenario H0, H1, H2, and H3 with low amounts of genetic replacement are very similar to the one observed in the modern sample. When the amount of replacement increases, then mismatch distributions tend to be multimodal and to show an excess of low numbers of differences between sequences when compared to the observed mismatch distribution.

Only scenarios H3 involving substantial genetic replacement (>25%) are able to produce more than 5% of simulations resulting in both unimodal mismatch distributions and genetic differentiation between the simulated Neolithic and modern samples larger than those observed, H3d (50% replacement) being the scenario with the largest proportion of compatible simulations (P_{uni} and $Fst_{sim>obs} = 24.6\%$).

4 | DISCUSSION AND CONCLUSION

The results presented here show that a substantial population replacement due to immigration between the Neolithic and the present may alter the shape of mismatched distributions in modern populations (scenario H3d and H3g in Figure 4). Increasing population replacement between those two periods tends to decrease the proportion of unimodal mismatch distributions and to increase the genetic differentiation between the Neolithic and the modern sample. Despite this opposite trend, we show intermediate situations of partial population replacement during the Bronze Age that are compatible with both observed mitochondrial patterns in Central Europe, namely a unimodal mismatch distribution in modern populations (Excoffier & Schneider, 1999) and high genetic differentiation between Neolithic and modern population samples (Bramanti et al., 2009). Consequently, a unimodal mismatch distribution in modern population does not oppose to a partial population turnover after the Neolithic transition. Our results therefore show that the hypothesis of a substential genomic contribution of people linked to the Yamnaya cultural complex in Central Europe during the Bronze Age is not only supported by paleogenomic data (Allentoft et al., 2015; Haak et al., 2015) but is also consistent with the observed patterns of mitochondrial diversity. Our simulation study therefore makes the link between results obtained both from modern (Currat & Excoffier, 2005; Excoffier & Schneider, 1999) and ancient (Bramanti et al., 2009; Haak et al., 2005; Silva et al., 2017) mitochondrial data.

Even though our simulations were sufficient to conclude that some scenario of migration during the Bronze Age are compatible with the observed patterns of mtDNA diversity, we raise caution in interpreting the situation this migration wave may have occurred, because a limited number of scenarios and parameter values have been explored here. Roughly, it seems that admixture rate (γ) values leading to a genetic replacement of approximately half of the Central European gene pool by immigrants populations after the Neolithic period is the most compatible with the observation (Table 3). However, the value of γ compatible with the observed data also depends on the other parameters that were fixed in the current study. Here, we decided to represent massive migrations from the steppes in the model because it was recently supported by paleogenomic studies (Haak et al., 2015), but we can imagine that a single or multiple immigration waves could have happened at other periods between the Neolithic and nowadays (Sokal, 1991). A more systematic exploration of the conditions of partial genetic replacement since the Neolithic transition till today through a model choice procedure like Approximate Bayesian Computation (e.g., Bertorelle et al., 2010) would thus be essential to get a more precise view on this question. Given the current debate among archeologists and paleogeneticists on the topic (e.g., Furholt, 2018; Haak et al., 2015; Heyd, 2017; Veeramah, 2018), there are many aspects of this complex period in western Eurasia which worth to be considered and explored using a modeling approach. Such investigation is beyond the scope of the current study but it would undeniably constitute its logical continuation. In particular, the use of multiple loci such as paleogenomic data (Mathieson et al., 2018; Olalde et al., 2018) could bring more power for model discrimination than a single locus investigation. In addition, the comparison between mitochondrial, autosomal and Y chromosome patterns could help to detect possible sex-specific pattern (e.g., Rasteiro & Chikhi, 2013).

Our results show that none of the investigated scenarios alternative to the immigration hypothesis are able to produce a genetic differentiation as large as the one observed at the mitochondrial level between Neolithic and modern populations from Central Europe ($Fst = 0.072$, see Section 2). We show that such a high genetic differentiation (Bramanti et al., 2009) cannot be reached without involving a genetic input from a differentiated population (Table 3). Scenarios involving genetic drift, demographic fluctuations, or drop following the Neolithic transition without genetic input from another area, do not shuffle allele frequencies sufficiently to create a genetic differentiation as the one observed on the mtDNA. We found that variations of population density affect only marginally the proportion of unimodal mismatch distribution and the *Fst* statistic. Even an extreme scenario of 90% demographic collapse during historical times is not sufficient to increase the simulated *Fst* within the range of the observed value. In the extreme cases of demographic collapses, we recorded no significant differences in nucleotidic diversity before (H1c = 0.01 ± 0.04, H2b = 0.009 ± 0.005) and during the bottleneck (H1c = 0.009 ± 0.04, H2b = 0.009 ± 0.02), neither in scenarios H1 nor in scenarios

H2. This implies that the large absolute population density after the Neolithic transition combined to the population structure prevents the loss of genetic diversity that would be caused by the bottleneck (Wakeley, 1999), even when the bottleneck is proportionally extremely large.

We also found that all scenarios, including simple population continuity, led to a substantial proportion (>5.2%) of simulations showing a simulated haplogroup frequency decline between the Neolithic and the modern period similar to the one experienced by N1a. It suggests that genetic drift in a subdivided population is not fully incompatible with the drop in frequency observed for N1a in Europe in a few thousand years (Brandt et al., 2015; Fu et al., 2012; Haak et al., 2005, 2015) even if its probability is quite low (<10%). The frequency drop of N1a is thus not indicative per se of population discontinuity during this time lapse. However, scenarios involving a partial population replacement during the Bronze Age show a much larger proportion of decrease in frequency of simulated haplogroup similar to N1a, thus going in the same direction as the other diversity patterns analyzed.

In conclusion, our investigation of the consequences of post-Neolithic demographic events in Central Europe on mitochondrial diversity using a spatially explicit modeling framework did not provide a plausible alternative explanation, but rather supported the current hypothesis of partial population replacement between the Neolithic and contemporary populations in this area. We showed that this hypothesis is compatible with the intrapopulation patterns of mitochondrial diversity in modern populations and that a migration wave from the Pontic steppes during the Bronze Age is the best explicative scenario, among those investigated, to the large genetic shift during this period in Central Europe. Even though our conclusions rely on a specific part of the genome that is transmitted only through the female line, they are in agreement with results obtained from ancient genome wide data (e.g., Allentoft et al., 2015; Haak et al., 2015). Further modeling studies would be required to better characterize the conditions of this genetic input through a more quantitative analysis.

ACKNOWLEDGMENTS

The authors would like to thank Jérémy Rio, Pascale Gerbault, and Claudio S. Quilodrán for a careful reading of the manuscript as well stimulating discussions on the subject, as well as Yann Sagon and Stephan Weber for computational support. The authors also thank two anonymous reviewers for helpful comments on a previous version of the manuscript. This work was supported by grants n° 31003A_156853 and n° 31003A_182577 (to M. C.) from the Swiss National Science Foundation. Open access funding provided by Université de Genève. Open Access Funding provided by Universite de Geneve.

CONFLICT OF INTEREST

The authors declare there is no conflict of interest.

AUTHOR CONTRIBUTIONS

Nicolas Broccard: Conceptualization (equal); formal analysis (lead); investigation (lead); methodology (equal); software (equal); writing – original draft (lead); writing – review and editing (supporting). **Nuno Miguel Silva:** Methodology (supporting); software (supporting); supervision (supporting); writing – review and editing (supporting). **Mathias Currat:** Conceptualization (lead); funding acquisition (lead); methodology (equal); project administration (lead); software (equal); supervision (lead); writing – review and editing (lead).

DATA AVAILABILITY STATEMENT

Data sharing is not applicable to this article as no new data were created or analyzed in this study.

ORCID

Mathias Currat https://orcid.org/0000-0001-5211-8922

REFERENCES

Allentoft, M. E., Sikora, M., Sjögren, K. G., Rasmussen, S., Rasmussen, M., Stenderup, J., Damgaard, P. B., Schroeder, H., Ahlström, T., Vinner, L., Malaspinas, A. S., Margaryan, A., Higham, T., Chivall, D., Lynnerup, N., Harvig, L., Baron, J., Della Casa, P., Dąbrowski, P., … Willerslev, E. (2015). Population genomics of bronze age Eurasia. *Nature*, *522*(7555), 167–172. https://doi.org/10.1038/nature14507

Alroy, J. (2001). A multispecies overkill simulation of the end-Pleistocene megafaunal mass extinction. *Science*, *292*(5523), 1893–1896.

Arenas, M., Francois, O., Currat, M., Ray, N., & Excoffier, L. (2013). Influence of admixture and paleolithic range contractions on current European diversity gradients. *Molecular Biology and Evolution*, *30*(1), 57–61. https://doi.org/10.1093/molbev/mss203

Baasner, A., & Madea, B. (2000). Sequence polymorphisms of the mitochondrial DNA control region in 100 German Caucasians. *Journal of Forensic Sciences*, *45*(6), 1343–1348.

Barbujani, G., Sokal, R. R., & Oden, N. L. (1995). Indo-European origins: A computer-simulation test of five hypotheses. *American Journal of Physical Anthropology*, *96*(2), 109–132.

Bardet, J.-P., & Dupâquier, J. (1997). *Histoire des populations de l'Europe*. Fayard.

Bertorelle, G., Benazzo, A., & Mona, S. (2010). ABC as a flexible framework to estimate demography over space and time: Some cons, many pros. *Molecular Ecology*, *19*(13), 2609–2625.

Biraben, J. N. (1979). Essay on the evolution of numbers of mankind. *Population*, *34*(1), 13–25.

Bocquet-Appel J.-P., Demars P.-Y. (2000). Population Kinetics in the Upper Palaeolithic in Western Europe. *Journal of Archaeological Science*, *27*(7), 551–570. https://doi.org/10.1006/jasc.1999.0471

Bocquet-Appel, J.-P., & Dubouloz, J. (2003). Traces paléoanthropologiques et archéologiques d'une transition démographique néolithique en Europe. *Bulletin de la société préhistorique française*, *100*(4), 699–714.

Bramanti, B., Thomas, M. G., Haak, W., Unterlaender, M., Jores, P., Tambets, K., Antanaitis-Jacobs, I., Haidle, M. N., Jankauskas, R., Kind, C.-J., Lueth, F., Terberger, T., Hiller, J., Matsumura, S., Forster, P., & Burger, J. (2009). Genetic discontinuity between local hunter-gatherers and Central Europe's first farmers. *Science*. *326*, 137–140. https://doi.org/10.1126/science.1176869

Brandt, G., Haak, W., Adler, C. J., Roth, C., Szécsényi-Nagy, A., Karimnia, S., Möller-Rieker, S., Meller, H., Ganslmeier, R., Friederich, S., Dresely, V., Nicklisch, N., Pickrell, J. K., Sirocko, F., Reich, D., Cooper, A., Alt, K. W., & Genographic Consortium. (2013). Ancient DNA reveals key stages in the formation of central European mitochondrial genetic diversity. *Science*, *342*(6155), 257–261. https://doi.org/10.1126/science.1241844

Brandt, G., Szecsenyi-Nagy, A., Roth, C., Alt, K. W., & Haak, W. (2015). Human paleogenetics of Europe - the known knowns and the known unknowns. *Journal of Human Evolution*, *79*, 73–92.

Chikhi, L., Nichols, R. A., Barbujani, G., & Beaumont, M. A. (2002). Y genetic data support the Neolithic demic diffusion model. *Proceedings of the National Academy of Sciences of the United States of America*, *99*(17), 11008–11013.

Comas, D., Calafell, F., Mateu, E., Perez-Lezaun, A., & Bertranpetit, J. (1996). Geographic variation in human mitochondrial DNA control region sequence: The population history of Turkey and its relationship to the European populations. *Molecular Biology and Evolution*, *13*(8), 1067–1077.

Currat, M., Arenas, M., Quilodran, C. S., Excoffier, L., & Ray, N. (2019). SPLATCHE3: Simulation of serial genetic data under spatially explicit evolutionary scenarios including long-distance dispersal. *Bioinformatics*, *35*(21), 4480–4483. https://doi.org/10.1093/bioinformatics/btz311

Currat, M., & Excoffier, L. (2005). The effect of the Neolithic expansion on European molecular diversity. *Proceedings of the Biological Sciences*, *272*(1564), 679–688. https://doi.org/10.1098/rspb.2004.2999

Currat, M., Ray, N., & Excoffier, L. (2004). SPLATCHE: A program to simulate genetic diversity taking into account environmental heterogeneity. *Molecular Ecology Notes*, *4*(1), 139–142. https://doi.org/10.1046/j.1471-8286.2003.00582.x

Currat, M., Ruedi, M., Petit, R. J., & Excoffier, L. (2008). The hidden side of invasions: Massive introgression by local genes. *Evolution*, *62*(8), 1908–1920. https://doi.org/10.1111/j.1558-5646.2008.00413.x

Deguilloux, M. F., Soler, L., Pemonge, M. H., Scarre, C., Joussaume, R., & Laporte, L. (2011). News from the west: Ancient DNA from a French megalithic burial chamber. *American Journal of Physical Anthropology*, *144*(1), 108–118. https://doi.org/10.1002/ajpa.21376

Demoule, J.-P. (2014). *Mais où sont passés les Indo-Européens?: Le mythe d'origine de l'Occident*. Seuil.

Eckert, E. A. (2000). The retreat of plague from Central Europe, 1640-1720: A geomedical approach. *Bulletin of the History of Medicine*, *74*(1), 1–28.

Excoffier, L. (2004). Patterns of DNA sequence diversity and genetic structure after a range expansion: Lessons from the infinite-Island model. *Molecular Ecology*, *13*(4), 853–864.

Excoffier, L., & Lischer, H. E. (2010). Arlequin suite ver 3.5: A new series of programs to perform population genetics analyses under Linux and Windows. *Molecular Ecology Resources*, *10*(3), 564–567. https://doi.org/10.1111/j.1755-0998.2010.02847.x

Excoffier, L., & Schneider, S. (1999). Why hunter-gatherer populations do not show signs of pleistocene demographic expansions. *Proceedings of the National Academy of Sciences of the United States of America*, *96*(19), 10597–10602.

Fu, Q., Rudan, P., Paabo, S., & Krause, J. (2012). Complete mitochondrial genomes reveal neolithic expansion into europe. *PLoS One*, *7*(3), e32473. https://doi.org/10.1371/journal.pone.0032473

Furholt, M. (2018). Massive migrations? The impact of recent aDNA studies on our view of third millennium Europe. *European Journal of Archaeology*, *21*, 159–191.

Gamba, C., Jones, E. R., Teasdale, M. D., McLaughlin, R. L., Gonzalez-Fortes, G., Mattiangeli, V., Domboróczki, L., Kovári, I., Pap, I., Anders, A., Whittle, A., Dani, J., Raczky, P., Higham, T. F. G., Hofreiter, M., Bradley, D. G., & Pinhasi, R. (2014). Genome flux and stasis in a five millennium transect of European prehistory. *Nature Communications*, *5*, 5257.

Gimbutas, M. (1979). The three waves of the Kurgan people into old world, 4500-2500 B.C. *Archives suisses d'anthropologie générale, Genève*, *43*(2), 113–137.

Gimbutas, M. (1991). *The civilization of the goddess: The world of old Europe*. San Francisco: Harper.

Haak, W., Balanovsky, O., Sanchez, J. J., Koshel, S., Zaporozhchenko, V., Adler, C. J., Members of the Genographic Consortium, Der Sarkissian, C., Brandt, G., Schwarz, C., Nicklisch, N., Dresely, V., Fritsch, B., Balanovska, E., Villems, R., Meller, H., Alt, K. W., & Cooper, A. (2010). Ancient DNA from European early neolithic farmers reveals their near eastern affinities. *PLoS Biology*, *8*(11), e1000536. https://doi.org/10.1371/journal.pbio.1000536

Haak, W., Forster, P., Bramanti, B., Matsumura, S., Brandt, G., Tänzer, M., Villems, R., Renfrew, C., Gronenborn, D., Alt, K. W., & Burger, J. (2005). Ancient DNA from the first European farmers in 7500-year-old Neolithic sites. *Science*, *310*(5750), 1016–1018.

Haak, W., Lazaridis, I., Patterson, N., Rohland, N., Mallick, S., Llamas, B., Brandt, G., Nordenfelt, S., Harney, E., Stewardson, K., Fu, Q., Mittnik, A., Bánffy, E., Economou, C., Francken, M., Friederich, S., Pena, R. G., Hallgren, F., Khartanovich, V., … Reich, D. (2015). Massive migration from the steppe was a source for indo-European languages in Europe. *Nature*, *522*(7555), 207–211.

Helgason, A., Hrafnkelsson, B., Gulcher, J. R., Ward, R., & Stefansson, K. (2003). A Populationwide coalescent analysis of Icelandic matrilineal and patrilineal genealogies: Evidence for a faster evolutionary rate of mtDNA lineages than Y chromosomes. *American Journal of Human Genetics*, *72*(0), 1370–1388.

Heyd, V. (2017). Kossinna's smile. *Antiquity*, *91*, 348–359.

Hofmanová, Z., Kreutzer, S., Hellenthal, G., Sell, C., Diekmann, Y., Díez-del-Molino, D., Van Dorp, L., López, S., Kousathanas, A., Link, V., Kirsanow, K., Cassidy, L. M., Martiniano, R., Strobel, M., Scheu, A., Kotsakis, K., Halstead, P., Triantaphyllou, S., Kyparissi-Apostolika, N., … Burger, J. (2016). Early farmers from across Europe directly descended from Neolithic Aegeans. *Proceedings of the National Academy of Sciences of the United States of America*, *113*(25), 6886–6891. https://doi.org/10.1073/pnas.1523951113

Kimura, M. (1953). Stepping-stone model of population. *Annual Report of National Institute of Genetics*, *3*, 62–63.

Klopfstein, S., Currat, M., & Excoffier, L. (2006). The fate of mutations surfing on the wave of a range expansion. *Molecular Biology and Evolution*, *23*(3), 482–490. https://doi.org/10.1093/molbev/msj057

Kohl, J., Paulsen, I., Laubach, T., Radtke, A., & von Haeseler, A. (2006). HvrBase++: A phylogenetic database for primate species. *Nucleic Acids Research*, *34*, D700–D704.

Lipson, M., Szécsényi-Nagy, A., Mallick, S., Pósa, A., Stégmár, B., Keerl, V., Rohland, N., Stewardson, K., Ferry, M., Michel, M., Oppenheimer, J., Broomandkhoshbacht, N., Harney, E., Nordenfelt, S., Llamas, B., Gusztáv Mende, B., Köhler, K., Oross, K., Bondár, M., … Reich, D. (2017). Parallel palaeogenomic transects reveal complex genetic history of early European farmers. *Nature*, *551*(7680), 368–372.

Livi Bacci, M. (1999). *La population dans l'histoire de l'Europe*. Seuil.

Mathieson, I., Alpaslan-Roodenberg, S., Posth, C., Szécsényi-Nagy, A., Rohland, N., Mallick, S., Olalde, I., Broomandkhoshbacht, N., Candilio, F., Cheronet, O., Fernandes, D., Ferry, M., Gamarra, B., Fortes, G. G., Haak, W., Harney, E., Jones, E., Keating, D., Krause-Kyora, B., … Reich, D. (2018). The genomic history of southeastern Europe. *Nature*, *555*, 197–203. https://doi.org/10.1038/nature25778

Mellars, P. (2006). A new radiocarbon revolution and the dispersal of modern humans in Eurasia. *Nature*, *439*(7079), 931–935.

Olalde, I., Brace, S., Allentoft, M. E., Armit, I., Kristiansen, K., Booth, T., Rohland, N., Mallick, S., Szécsényi-Nagy, A., Mittnik, A., Altena, E., Lipson, M., Lazaridis, I., Harper, T. K., Patterson, N., Broomandkhoshbacht, N., Diekmann, Y., Faltyskova, Z., Fernandes, D., … Reich, D. (2018). The beaker phenomenon and the genomic transformation of Northwest Europe. *Nature*, *555*, 190–196. https://doi.org/10.1038/nature25738

Ortega-Del Vecchyo, D., & Slatkin, M. (2019). FST between archaic and present-day samples. *Heredity (Edinb).*, *122*, 711–718. https://doi.org/10.1038/s41437-018-0169-8

Palanichamy, M. G., Zhang, C. L., Mitra, B., Malyarchuk, B., Derenko, M., Chaudhuri, T. K., & Zhang, Y. P. (2010). Mitochondrial haplogroup N1a phylogeography, with implication to the origin of European farmers. *BMC Evolutionary Biology*, *10*, 304. https://doi.org/10.1186/1471-2148-10-304

Quilodrán C. S., Tsoupas A., & Currat M. (2020). The spatial signature of introgression after a biological invasion with hybridization. *Front. Ecol. Evol*, *8*, 569620. https://doi.org/10.3389/fevo.2020.569620

Rasteiro, R., Bouttier, P. A., Sousa, V. C., & Chikhi, L. (2012). Investigating sex-biased migration during the Neolithic transition in Europe, using an explicit spatial simulation framework. *Proceedings of the Biological Sciences*, *279*(1737), 2409–2416. https://doi.org/10.1098/rspb.2011.2323

Rasteiro, R., & Chikhi, L. (2013). Female and male perspectives on the Neolithic transition in Europe: Clues from ancient and modern genetic data. *PLoS One*, *8*(4), e60944. https://doi.org/10.1371/journal.pone.0060944

Ray, N., Currat, M., & Excoffier, L. (2003). Intra-deme molecular diversity in spatially expanding populations. *Molecular Biology and Evolution*, *20*(1), 76–86. https://doi.org/10.1093/molbev/msg009

Rendine, S., Piazza, A., & Cavalli-Sforza, L. (1986). Simulation and separation by principal components of multiple demic expansions in Europe. *The American Naturalist*, *128*(5), 681–706.

Richards, M., Macaulay, V., Hickey, E., Vega, E., Sykes, B., Guida, V., Rengo, C., Sellitto, D., Cruciani, F., Kivisild, T., Villems, R., Thomas, M., Rychkov, S., Rychkov, O., Rychkov, Y., Gölge, M., Dimitrov, D., Hill, E., Bradley, D., … Bandelt, H. J. (2000). Tracing European founder lineages in the near eastern mtDNA pool. *American Journal of Human Genetics*, *67*(5), 1251–1276.

Rieux, A., Eriksson, A., Li, M. K., Sobkowiak, B., Weinert, L. A., Warmuth, V., Ruiz-Linares, A., Manica, A., & Balloux, F. (2014). Improved calibration of the human mitochondrial clock using ancient genomes. *Molecular Biology and Evolution*, *31*(10), 2780–2792.

Rivollat, M., Mendisco, F., Pemonge, M. H., Safi, A., Saint-Marc, D., Brémond, A., Couture-Veschambre, C., Rottier, S., & Deguilloux, M. F. (2015). When the waves of European Neolithization met: First paleogenetic evidence from early farmers in the southern Paris Basin. *PLoS One*, *10*(4), e0125521. https://doi.org/10.1371/journal.pone.0125521

Rivollat, M., Réveillas, H., Mendisco, F., Pemonge, M. H., Justeau, P., Couture, C., Lefranc, P., Féliu, C., & Deguilloux, M. F. (2016). Ancient mitochondrial DNA from the middle neolithic necropolis of Obernai extends the genetic influence of the LBK to west of the Rhine. *American Journal of Physical Anthropology*, *161*, 522–529. https://doi.org/10.1002/ajpa.23055

Rogers, A. R., & Harpending, H. (1992). Population growth makes waves in the distribution of pairwise genetic differences. *Molecular Biology and Evolution*, *9*(3), 552–569.

Shennan, S., Downey, S. S., Timpson, A., Edinborough, K., Colledge, S., Kerig, T., Manning, K., & Thomas, M. G. (2013). Regional population collapse followed initial agriculture booms in mid-Holocene Europe. *Nature Communications*, *4*, 2486. https://doi.org/10.1038/ncomms3486

Silva, N. M., Rio, J., & Currat, M. (2017). Investigating population continuity with ancient DNA under a spatially explicit simulation framework. *BMC Genetics*, *18*(1), 114. https://doi.org/10.1186/s12863-017-0575-6

Silva, N. M., Rio, J., Kreutzer, S., Papageorgopoulou, C., & Currat, M. (2018). Bayesian estimation of partial population continuity using ancient DNA and spatially explicit simulations. *Evolutionary Applications*, *11*(9), 1642–1655. https://doi.org/10.1111/eva.12655

Sokal, R. R. (1991). Ancient movement patterns determine modern genetic variances in Europe. *Human Biology*, *63*(5), 589–606.

Stamatakis, A. (2014). RAxML version 8: A tool for phylogenetic analysis and post-analysis of large phylogenies. *Bioinformatics*, *30*(9), 1312–1313.

Steele J., Adams J., & Sluckin T. (1998). Modelling Paleoindian dispersals. *World Archaeology*, *30*(2), 286–305. https://doi.org/10.1080/00438243.1998.9980411

Szécsényi-Nagy, A., Brandt, G., Haak, W., Keerl, V., Jakucs, J., Möller-Rieker, S., Köhler, K., Gusztáv Mende, B., Oross, K., Marton, T., Osztás, A., Kiss, V., Fecher, M., Pálfi, G., Molnár, E., Sebők, K., Czene, A., Paluch, T., Šlaus, M., Novak, M., …, Kurt, W. (2015). Tracing the genetic origin of Europe's first farmers reveals insights into their social organization. *Proceedings of the Royal Society B-Biological Sciences*, *282*(1805), 20150339.

Tremblay, M., & Vezina, H. (2000). New estimates of intergenerational time intervals for the calculation of age and origins of mutations. *American Journal of Human Genetics*, *66*(2), 651–658.

Unterlander, M., Palstra, F., Lazaridis, I., Pilipenko, A., Hofmanova, Z., Gross, M., Sell, C., Blöcher, J., Kirsanow, K., Rohland, N., Rieger, B., Kaiser, E., Schier, W., Pozdniakov, D., Khokhlov, A., Georges, M., Wilde, S., Powell, A., Heyer, E., … Burger, J. (2017). Ancestry and demography and descendants of iron age nomads of the Eurasian steppe. *Nature Communications*, *8*, 14615. https://doi.org/10.1038/ncomms14615

van Oven, M., & Kayser, M. (2009). Updated comprehensive phylogenetic tree of global human mitochondrial DNA variation. *Human Mutation*, *30*(2), E386–E394. https://doi.org/10.1002/humu.20921

Veeramah, K. R. (2018). The importance of fine-scale studies for integrating paleogenomics and archaeology. *Current Opinion in Genetics & Development*, *53*, 83–89.

Wakeley, J. (1999). Nonequilibrium migration in human history. *Genetics*, *153*(4), 1863–1871.

Zimmermann, A., Hilpert, J., & Wendt, K. P. (2009). Estimations of population density for selected periods between the Neolithic and AD 1800. *Human Biology*, *81*(2–3), 357–380.

How to cite this article: Broccard, N., Silva, N. M., & Currat, M. (2022). Simulated patterns of mitochondrial diversity are consistent with partial population turnover in Bronze Age Central Europe. *American Journal of Biological Anthropology*, *177*(1), 134–146. https://doi.org/10.1002/ajpa.24431